

# 50 GHz Piezoelectric Acoustic Filter

**Omar Barrera (Student Member, IEEE), Jack Kramer (Student Member, IEEE),  
Lezli Matto, Vakhtang Chulukhadze (Student Member, IEEE), Sinwoo Cho (Student  
Member, IEEE), Michael Liao, Mark S. Goorsky, and Ruochen Lu (Senior Member, IEEE)**  
The University of Texas at Austin, Austin, TX USA; University of California, Los Angeles, Los Angeles, CA, USA

CORRESPONDING AUTHOR: Omar Barrera (e-mail: [omarb@utexas.edu](mailto:omarb@utexas.edu)).

This work was supported by DARPA Compact Front-End Filters at the EElement-Level (COFFEE)

---

**ABSTRACT** This paper presents significant frequency scaling of acoustic filter technology to 50 GHz. This achievement is enabled by the P3F LiNbO<sub>3</sub> multilayer stack, in which piezoelectric thin-films of alternating orientations are transferred in sequence, thereby allowing efficient exploitation of high-order modes with high quality factor ( $Q$ ) and coupling coefficient ( $k^2$ ) in a thicker piezoelectric stack. The demonstrated filter is comprised of twelfth-order symmetric (S12) mode lateral-field-excited bulk acoustic wave resonators (XBARs), built on a 4-layer periodically poled piezoelectric (P3F) 128° Y-cut lithium niobate (LiNbO<sub>3</sub>) stack. The filter exhibits 3.3 dB insertion loss (IL) and a fractional bandwidth (FBW) of 2.9%. The miniature design, with a footprint of 0.36 mm<sup>2</sup>, makes it promising for future wireless front-end applications. These results represent the highest frequency acoustic filters reported to date, setting a new benchmark in piezoelectric filter technology. Upon further development, the platform could enable filters further into the FR2 range, essential for next-generation communication systems.

**INDEX TERMS** Acoustic filters, lithium niobate, millimeter-wave (mmWave), periodically poled piezoelectric film (P3F), piezoelectric devices, thin-film devices

---

## I. INTRODUCTION

The rapid proliferation of smartphones created a ripple effect that led to a growing demand for larger data transfer speeds, and consequently, the need for higher operating frequencies [1]. A key element that has contributed to the success of the smartphone is the introduction of miniature acoustic filters [2], [3]. In an acoustic device, electrical signals are converted back and forth to mechanical vibrations, which propagate with relatively low attenuation [4], [5]. Additionally, acoustic wavelengths are several orders of magnitude smaller than those of electromagnetic (EM) waves, enabling efficient energy transfer and compact design [6]. These characteristics make acoustic wave devices ideal for meeting the stringent size and performance requirements of radio frequency (RF) front end for modern mobile communication systems (Fig. 1). With the demand for data transfer rates projected to keep

rising [7], acoustic devices are expected to remain the backbone of RF mobile filtering [8]. Two types of acoustic resonator technologies are often employed in acoustic filters, namely surface acoustic waves (SAW) and bulk acoustic waves (BAW) resonators. The latter is the preferred method for higher frequency applications, since BAW resonators maintain better electromechanical coupling ( $k^2$ ) and quality factors ( $Q$ ), required for high-performance filters [9]. Frequency scaling in BAW devices is implemented by reducing the thickness of the piezoelectric layer. While straightforward in theory, practical limitations exist due to fabrication constraints. Moreover, ultra-thin film devices are difficult to implement in 50Ω systems, and high acoustic damping results in reduced device performance [10]. As a result, commercially available devices based on aluminum nitride/scandium aluminum nitride (AlN/ScAlN) have remained limited at sub-6 GHz frequencies [11], [12].

This work is licensed under a Creative Commons Attribution 4.0 License. For more information, see <https://creativecommons.org/licenses/by/4.0/>

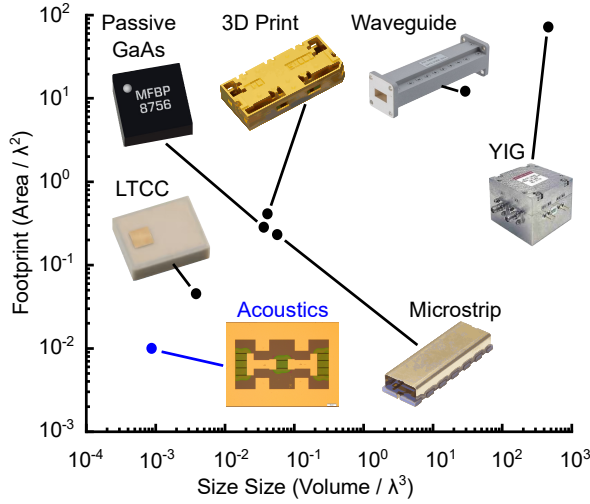


Fig.1 Dimension comparison between different high-frequency filter technologies.

Table I State-of-the-Art Acoustic Filters above 10 GHz

Reference	$f_c$ (GHz)	$IL$ (dB)	$FBW$ (%)	Rejection (dB)
[29]	9.96	0.76	5.7	3.8
[28]	17.4	3.3	3.4	16.6
[20]	19.0	8.0	2.4	13.0
[19]	23.5	2.4	18.2	13.0
[25]	23.8	1.5	19.4	12.1
[21]	38.7	5.6	17.6	15.8
<b>This work</b>	<b>50.1</b>	<b>3.3</b>	<b>2.9</b>	<b>15.2</b>

Recently, transferred thin-film lithium niobate ( $\text{LiNbO}_3$ ) has been proposed as a new BAW platform [13]–[15]. These laterally excited resonators, known commercially as lateral-field-excited bulk acoustic wave resonator (XBAR) [16], excite the first anti-symmetric (A1) mode and provide large  $k^2$  [17], operating deep into the mmWave frequency range [18]. The platform has been successfully used to demonstrate high-performance acoustic filters on single layer  $\text{LiNbO}_3$  [19], [20]. Ultra-thin-film devices have also been reported, though with lower performance, highlighting the limitations of using single-layer stacks for large frequency scaling [21], [22].

To overcome the limitations of the single-layer approach, multi-layer periodically poled piezoelectric film (P3F) devices have been demonstrated in  $\text{LiNbO}_3$  [23]–[25], as well as on  $\text{AlN}/\text{ScAlN}$ -based devices [26]–[30]. This approach enables larger  $k^2 \cdot Q$  metrics at high frequencies, along with the added benefits of thicker film's capacitance density for  $50\Omega$  impedance matching.

In this article, we report a 4-layer P3F filter at 50 GHz, significantly exceeding the current state of the art (Table I). The P3F filter's resonators utilize the 12<sup>th</sup> symmetric mode (S12) and exhibit  $Q_s$  of 22 and 52,  $k^2$  of 2.56% and 4.12% for the shunt and series resonators, respectively. The fabricated filter is centered at 50.1 GHz, with a low insertion loss ( $IL$ ) of 3.3 dB and a 3-dB fractional

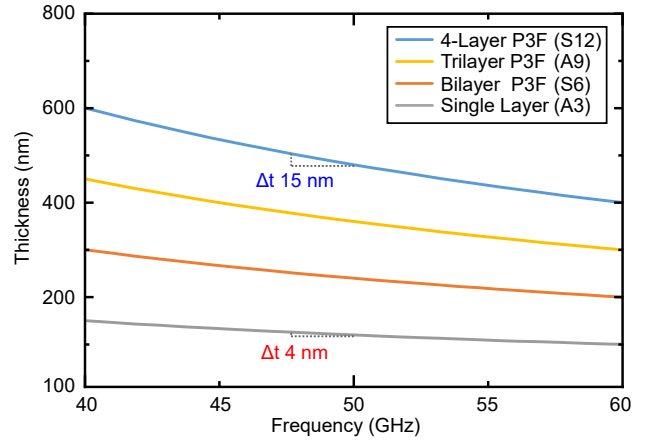


Fig. 2 Dispersion of A3 in  $\text{LiNbO}_3$  XBARs and higher-order overtones in  $\text{LiNbO}_3$  at 40-60 GHz, highlighting the relaxed requirement of fine trimming to realize the frequency shift for shunt and series resonators in thicker stacks, which is supported by multi-layer P3F  $\text{LiNbO}_3$  for high FoM resonators.

bandwidth ( $FBW$ ) of 2.9%. These results represent the highest frequency reported in the field to date, demonstrating piezoelectric filters deep into the FR2 bands for the first time [31].

## II. ANALYSIS AND DESIGN

The design of a mmWave acoustic filter at 50 GHz requires an appropriate piezoelectric material stack to support the desired acoustic resonances. A single-layer film working at the first symmetric (A1) mode would need to be approximately 40 nm thick, placing it in the lossy ultra-thin film regime. To overcome this task, utilizing a device employing its higher-order harmonics in a thicker stack presents a more practical solution. The calculated frequency response vs thickness for the proposed solution is displayed in Fig. 2 for a number of stacks. The frequency response has been calculated as [32]:

$$f = \sqrt{(v_\lambda/\lambda)^2 + (N_h v_h/2h)^2} \quad (1)$$

where  $\lambda$  is the lateral wavelength,  $v_\lambda$  is the acoustic velocity in the lateral dimension,  $h$  is the thickness,  $v_h$  is the acoustic velocity in the thickness direction, and  $N_h$  is the order mode.

Based on Eq. 1, a single-layer stack employing the A3 mode at 50 GHz could be fabricated using a film of 110 nm thick (Fig. 2), which is within the reach of current fabrication capabilities. However, fine control over the frequency shift ( $\Delta f$ ) for implementing shunt and series resonators poses a challenge: even a mere  $\pm 1$  nm deviation can significantly degrade the filter performance, as the design requires a 4 nm thickness difference. One can further increase the mode order for more tolerance, but the  $k^2$  of those resonators will be too low for filters.

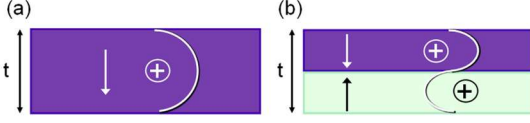


Fig. 3 Working principle of P3F stacks (a) single layer with thickness  $t$  operating at a frequency  $f$  and (b) bi-layer with thickness  $t$  and individual layers in opposite orientations. This mode operates at a frequency  $2f$ , with the same coupling coefficient as the fundamental in a single layer.

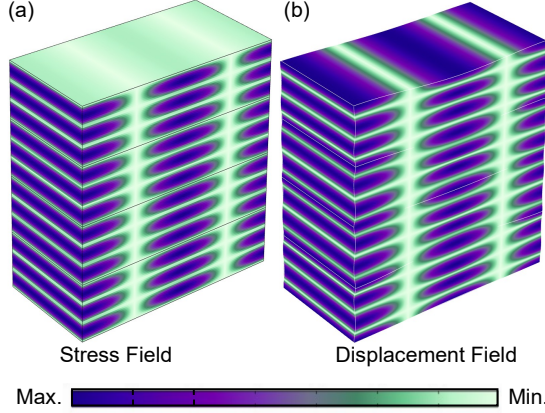


Fig.4 FEA simulated (a) von Mises stress distribution and (b) displacement field of S12 mode in 4-layer P3F LiNbO<sub>3</sub>.

As explained in the introduction, P3F layers with alternating piezoelectric orientations (Fig. 3) allow higher-order overtone operation without losing  $k^2$ . Consequently, a 4-layer P3F stack operating at the S12 mode can be fabricated with individual layers of 110 nm, resulting in a total thickness of 440 nm. This stack allows for a more manufacturable difference of 15 nm needed to realize the required frequency shift, well within current ion-mill trim processing tolerances. The added volume of a thicker stack also improves acoustic energy confinement, leading to higher resonator  $Q$ , and hence, improved filter  $IL$ . Moreover, the increased thickness offers larger capacitance density, reducing the footprint of the devices. As such, a 4-layer P3F stack is selected for this work.

The design process begins by simulating the stack response using COMSOL finite element analysis (FEA). The resulting stress and displacement distributions for the 4-layer stack are shown in Fig. 4. The stress profile (Fig. 4a) shows a total of 12 alternating stress maxima along the thickness direction, indicative of the S12 mode. In terms of displacement (Fig. 4b), particle motion is observed to alternate direction in the longitudinal axis, which is typical of shear wave propagation.

The thickness difference for the resonators is selected from the FEA results in order to obtain the required frequency shift to realize the filter passband. The resonator design is largely based on the work reported in [18]. The design values are listed in Table II. A thickness difference

Table II. Resonator Design Parameters

Resonator	LiNbO <sub>3</sub> Thickness (nm)	$\lambda$ ( $\mu$ m)	$f_s$ (GHz)	$C_0$ (fF)	$Q$	$k^2$ (%)
Series	427	8	49.6	37	80	4.8
Shunt	440	8	47.7	80	80	7.5

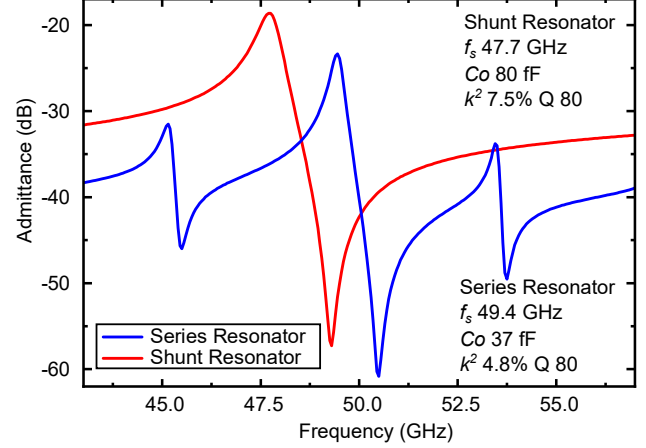


Fig. 5 Simulated shunt and series resonator admittance magnitude

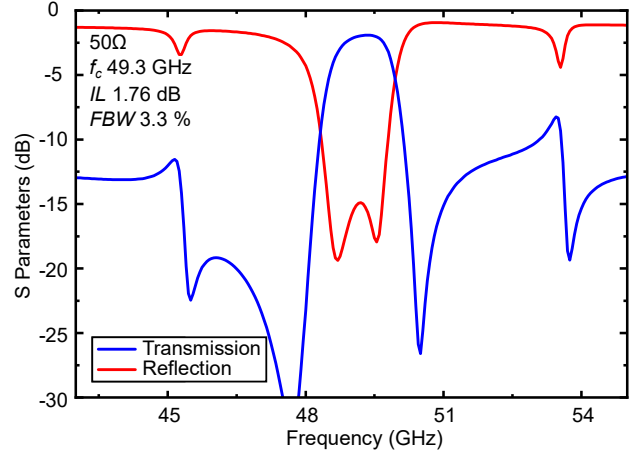


Fig. 6 Simulated 3<sup>rd</sup>-order ladder filter transmission and reflection.

of 13 nm is chosen here for the LiNbO<sub>3</sub> thickness trimming, slightly different from that calculated in Eq. 1, as the electrodes contribute to the resonance. The frequency domain FEA is shown in Fig. 5. For the shunt resonator, S12 is the only tone in the spectrum. For the series resonator, since the top layer will be trimmed down for the frequency shifting in filters, the adjacent 11<sup>th</sup>-order antisymmetric (A11) and 13<sup>th</sup>-order antisymmetric (A13) modes are excited, as the stress field will no longer be fully cancelled due to nonuniform thickness [33], but still with much lower coupling.

The filter design is implemented by exporting the resonator performance from COMSOL and utilizing the

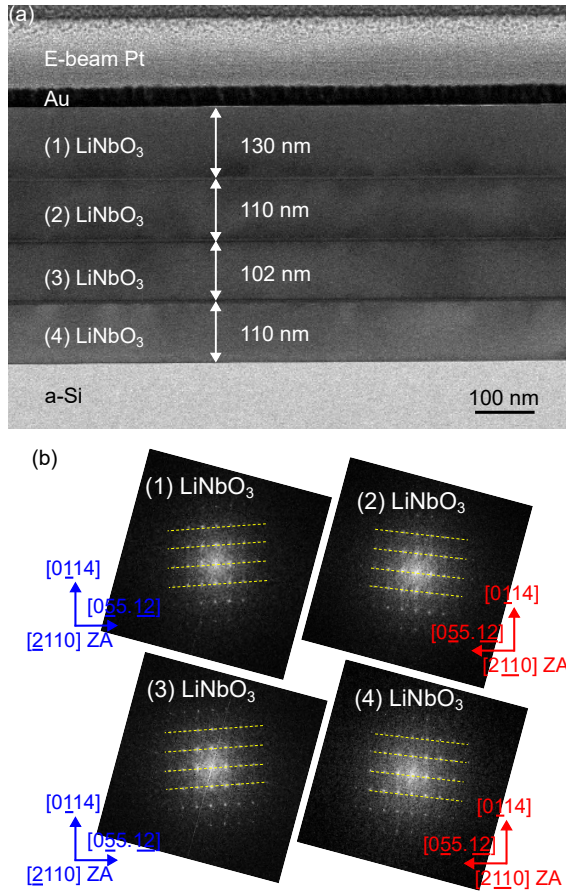


Fig. 7. (a) Cross-sectional BF-STEM image of the 4-Layer P3F LiNbO<sub>3</sub> and (b) FFT extraction of the reciprocal lattice of each layer.

modified Butterworth-Van Dyke (mBVD) model to fit the performance. The resulting parameters are then used to simulate a third-order ladder filter response in Keysight Advanced Design System. The resonator parameters are optimized numerically to minimize  $IL$  for a 50 $\Omega$  filter, assuming a moderate  $Q$  of 80 based on prior measurement results. The simulated filter response (Fig. 6) is centered at 49.3 GHz, exhibiting a low  $IL$  of 1.7 dB and a 3-dB  $FBW$  of 3.3%, indicating a promising mmWave acoustic filter. The simulated out-of-band (OoB) rejection is around 12 dB, except for the tones introduced by A11 and A13 in the series resonator, as discussed above. These modes can be eventually mitigated by starting with a film with slightly thicker top layers, but we will start with a uniform thickness P3F stack for the prototype purpose.

### III. FABRICATION AND RESULTS

The stack is provided by NGK Insulators Ltd. It consists of a 4-layer P3F LiNbO<sub>3</sub> on 1  $\mu$ m amorphous silicon (a-Si) layer, on top of a 500  $\mu$ m sapphire substrate. Each adjacent thin layer of LiNbO<sub>3</sub> is rotated 180° about the material X axis and in-plane 180° with respect to adjacent layers to provide a periodically poled piezoelectric film (P3F). Bright-field scanning transmission microscopy (BF-

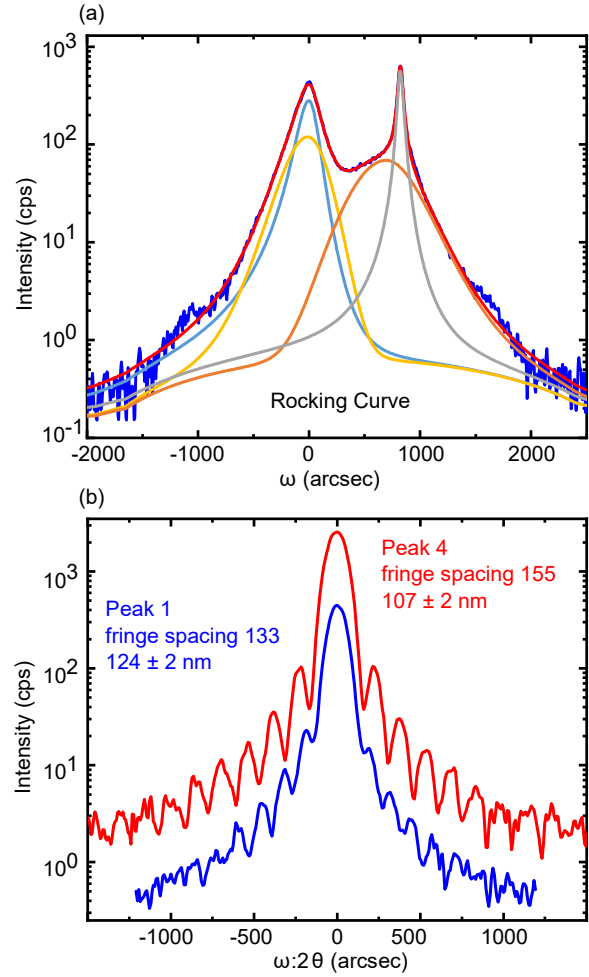


Figure 8. (a) Deconvoluted Peaks associated with each layer in the four layer stack. (b) Thickness fringes for peaks 1 and 4.

STEM) [Fig.7(a)] shows the four distinct LiNbO<sub>3</sub> layers. The layers show only very small thickness differences, which could otherwise introduce additional modes in the frequency response of resonators [34], but are sufficient for the 50 GHz filter prototype. FFT extractions of the lattice for each layer are used to verify in-plane crystal orientation, showing alternating patterns for each subsequent layer. Along this  $[2\bar{1}10]$  zone axis of the LiNbO<sub>3</sub> layers, the in-plane lattice rotations are clearly visible and confirm the  $180 \pm 3^\circ$  twist from layer to layer [Fig.7 (b)].

High resolution X-ray diffraction (XRD) characterization was performed with a Bruker-JV D1 X-ray diffractometer using triple-axis diffraction (TAD), which provides a non-destructive means to determine materials parameters of the layers. The TAD rocking curves of the symmetric (0114) reflection were used to quantify lattice tilt and mosaicity of the individual layers, and  $\omega:2\theta$  scans were used to measure layer thickness values. Peaks were separated along the rocking curve [Fig. 8(a)] scanning axis, and the peaks of each layer were deconvoluted by peak fitting. The measured peak widths FWHM of layers 1, 2, 3,



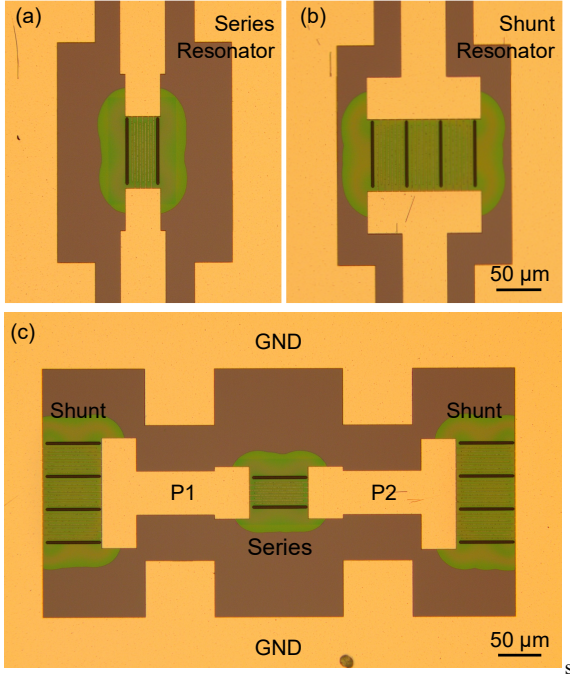


Fig. 9 Optical image of fabricated resonator testbed devices and also the 50 GHz filter.

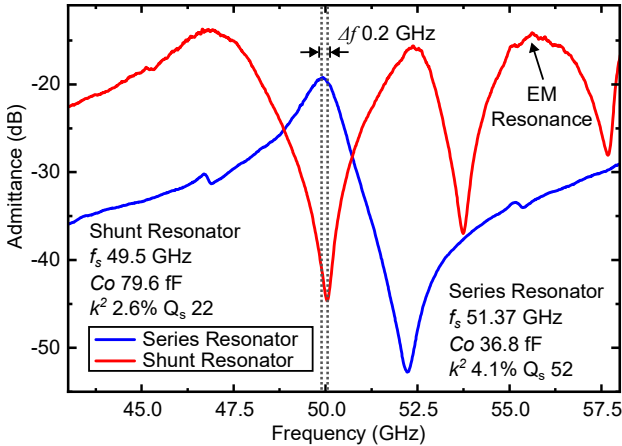


Fig. 10 Measured admittance magnitude of standalone resonators.

4 were 170°, 360°, 570° and 50°, respectively. The broader numbers observed are attributed to low-intensity peaks, introducing a degree of uncertainty that will be investigated in future works. Broader FWHM in the rocking curve corresponds to lattice tilt and mosaicity – these values were comparable to those from our prior publications. Fringe spacings from the  $\omega:2\theta$  scans [Fig. 8 (b)] were measured to determine thicknesses of two of the layers, which were found to be ~124 nm for peak 1, corresponding to layer 1 measured with STEM, and ~107 nm for peak 4, corresponding to layer 4 measured with STEM. The other two peaks did not exhibit enough intensity to resolve the thickness fringes.

Filter fabrication begins by defining local regions lithographically across a sample of 2.1 by 1.9 cm in dimensions. These regions are then selectively thinned by 13 nm using ion beam-assisted argon etching (ion-beam). The etched areas serve as a platform for the series resonators, with the thickness difference providing the required  $\Delta f$ . This process has been demonstrated to maintain surface roughness following the etch [35]. Following, the metal layer is defined for electrodes and interconnects using electron beam lithography (EBL). Aluminum (Al) is deposited in two stages by evaporation: first, a 350nm layer is deposited for both electrodes and interconnects, followed by an additional 350 nm for interconnects only, to enhance measurement robustness. Next, etch windows are patterned with EBL and etched deep into the aSi layer using ion-milling. Finally, the resonators are suspended using a silicon selective etch via xenon difluoride ( $\text{XeF}_2$ ). The optical images of the fabricated filter and resonators are shown in Fig. 9.

The devices are measured using a Keysight vector network analyzer (VNA) in air at a power level of -15 dBm. A short-open-load-through (SOLT) method was used to calibrate the response at the input of the devices. The resonator's admittance magnitude is displayed in Fig. 10, the frequency offset  $\Delta f$  between resonators shows good agreement with the values predicted from the dispersion analysis, validating the selection of the P3F stack. Additional acoustics modes are observed in the frequency response and are a result of thickness mismatches between layers. Furthermore, a resonance of EM nature is observed in the shunt resonator, arising from parasitic inductances in the layout.

The measured filter response, presented in Fig. 11, exhibits a passband centered at 50.1 GHz with an IL of 3.3 dB and a 3-dB FBW of 2.9%. These results are in agreement with the simulation response, demonstrating an effective utilization of an overtone in the P3F resonator stack to achieve a filter with a passband response in the upper FR2 frequency range. In comparison to other filter technologies at similar frequencies (Fig. 1) [36]–[41], this device features a bandpass response over a miniature footprint of 0.36 mm<sup>2</sup>, and a volume of 0.19 mm<sup>3</sup>, as predicted by the intrinsic short wavelength of the acoustic technology. This paper marks the first demonstration of piezoelectric acoustic filter technology at 50 GHz, compared to the state of the art (SoA) plotted in Fig. 12 and Table 1. Upon development, especially in lowering IL and providing higher OoB with closely integrated EM structures, such acoustic elements could provide new options for future mmWave front-end microsystems.

#### IV. CONCLUSIONS

We have presented the analysis, design, and implementation of an acoustic filter centered at 50 GHz, marking a significant advancement in frequency scaling.

This achievement is made possible by a four-layer P3F LiNbO<sub>3</sub> resonator stack that effectively harnesses the S12 overtone. The results demonstrated represent the highest operating frequency reported for acoustic filters to date, establishing a new benchmark in piezoelectric filter technology.

## ACKNOWLEDGMENT

The authors thank the DARPA COFFEE program for funding support, and Dr. Ben Griffin, Dr. Todd Bauer, and Dr. Zachary Fishman for helpful discussions. The authors also thank NSF CAREER: Radio Frequency Piezoelectric Acoustic Microsystems for Efficient and Adaptive Front-End Signal Processing.

## REFERENCES

- [1] S. Mahon, "The 5G Effect on RF Filter Technologies," *IEEE Transactions on Semiconductor Manufacturing*, vol. 30, no. 4, 2017.
- [2] R. Ruby, "A Snapshot in Time: The Future in Filters for Cell Phones," *IEEE Microw Mag*, vol. 16, no. 7, pp. 46–59, 2015.
- [3] A. Link and P. Warder, "Golden age for filter design: Innovative and proven approaches for acoustic filter, duplexer, and multiplexer design," *IEEE Microw Mag*, vol. 16, no. 7, 2015.
- [4] B. A. Auld and R. E. Green, "Acoustic Fields and Waves in Solids: Two Volumes," *Phys Today*, vol. 27, no. 10, 1974.
- [5] Warren P. Mason, *Electromechanical Transducers and Wave Filters*. 1948.
- [6] K. Hashimoto, *RF bulk acoustic wave filters for communications*, vol. 66. 2009.
- [7] INC. NTT DOCOMO, "5G Evolution and 6G - White Paper," *Distribution*, no. January, 2020.
- [8] A. Hagelauer et al., "From Microwave Acoustic Filters to Millimeter-Wave Operation and New Applications," *IEEE Journal of Microwaves*, vol. 3, no. 1, pp. 484–508, 2023.
- [9] J. F. Rosenbaum, *Bulk Acoustic Wave Theory and Devices*. Artech House, 1988.
- [10] M. Aljoumayy, R. Rothmund, M. Schaefer, and W. Heeren, "5G BAW Technology: Challenges and Solutions," in *2022 IEEE 22nd Annual Wireless and Microwave Technology Conference, WAMICON 2022*, 2022.
- [11] S. Gong, R. Lu, Y. Yang, L. Gao, and A. E. Hassanien, "Microwave Acoustic Devices: Recent Advances and Outlook," *IEEE Journal of Microwaves*, vol. 1, no. 2, pp. 601–609, 2021.
- [12] C. Cassella, Y. Hui, Z. Qian, G. Hummel, and M. Rinaldi, "Aluminum Nitride Cross-Sectional Lamé Mode Resonators," *Journal of Microelectromechanical Systems*, vol. 25, no. 2, 2016.
- [13] M. Kadota and T. Ogami, "5.4 GHz Lamb wave resonator on LiNbO<sub>3</sub> thin crystal plate and its application," *Jpn J Appl Phys*, vol. 50, no. 7 PART 2, 2011.
- [14] K. Mizutani and K. Toda, "Analysis of lamb wave propagation characteristics in rotated Y-cut X-propagation LiNbO<sub>3</sub> plates," *Electronics and Communications in Japan (Part I: Communications)*, vol. 69, no. 4, 1986.
- [15] V. Plessky et al., "Laterally excited bulk wave resonators (XBARs) based on thin Lithium Niobate platelet for 5GHz and 13 GHz filters," in *IEEE MTT-S International Microwave Symposium Digest*, 2019.
- [16] J. Koulakis et al., "XBAR physics and next generation filter design," in *IEEE International Ultrasonics Symposium, IUS*, 2021.
- [17] R. Lu, Y. Yang, S. Link, and S. Gong, "Al resonators in 128° Y-cut Lithium Niobate with Electromechanical Coupling of 46.4%," *Journal of Microelectromechanical Systems*, 2020.
- [18] J. Kramer et al., "57 GHz Acoustic Resonator with k<sub>2</sub> of 7.3 % and Q of 56 in Thin-Film Lithium Niobate," in *Technical Digest - International Electron Devices Meeting, IEDM*, 2022.
- [19] O. Barrera et al., "Thin-Film Lithium Niobate Acoustic Filter at 23.5 GHz with 2.38 dB IL and 18.2% FBW," *Journal of Microelectromechanical Systems*, Jul. 2023.
- [20] L. Gao, Y. Yang, and S. Gong, "Wideband hybrid monolithic lithium niobate acoustic filter in the K-band," *IEEE Trans Ultrason Ferroelectr Freq Control*, vol. 68, no. 4, pp. 1408–1417, 2020.
- [21] O. Barrera, S. Cho, J. Kramer, V. Chulukhadze, J. Campbell, and R. Lu, "38.7 GHz Thin Film Lithium Niobate Acoustic Filter," in *2024 IEEE International Microwave Filter Workshop, IMFW 2024*, 2024.
- [22] Z. Schaffer et al., "A Solidly Mounted 55 GHz Overmoded Bulk Acoustic Resonator," in *2023 IEEE International Ultrasonics Symposium (IUS)*, 2003.
- [23] J. Kramer et al., "Thin-Film Lithium Niobate Acoustic Resonator with High Q of 237 and k<sub>2</sub> of 5.1% at 50.74 GHz," in *IEEE International Frequency Control Symposium (IFCS)*, 2023.
- [24] J. Kramer et al., "Trilayer Periodically Poled Piezoelectric Film Lithium Niobate Resonator," in *IEEE International Ultrasonics Symposium, IUS*, 2023.
- [25] S. Cho et al., "23.8-GHz Acoustic Filter in Periodically Poled Piezoelectric Film Lithium Niobate With 1.52-dB IL and 19.4% FBW," *IEEE Microwave and Wireless Technology Letters*, 2024.
- [26] Izhar et al., "A K-Band Bulk Acoustic Wave Resonator Using Periodically Poled Al<sub>0.72</sub>Sc<sub>0.28</sub>N," *IEEE Electron Device Letters*, vol. 44, no. 7, 2023.
- [27] S. Nam, W. Peng, P. Wang, D. Wang, Z. Mi, and A. Mortazawi, "A mm-Wave Trilayer AlN/ScAlN/AlN Higher Order Mode FBAR," *IEEE Microwave and Wireless Technology Letters*, vol. 33, no. 6, 2023.
- [28] Izhar et al., "Periodically poled aluminum scandium nitride bulk acoustic wave resonators and filters for communications in the 6G era," *Microsyst Nanoeng*, vol. 11, no. 1, p. 19, 2025.
- [29] G. Giribaldi, L. Colombo, P. Simeoni, and M. Rinaldi, "Compact and wideband nanoacoustic pass-band filters for future 5G and 6G cellular radios," *Nat Commun*, vol. 15, no. 1, 2024.
- [30] R. Vetury et al., "A Manufacturable AlScN Periodically Polarized Piezoelectric Film Bulk Acoustic Wave Resonator (AlScN P3F BAW) Operating in Overtone Mode at X and Ku Band," in *IEEE MTT-S International Microwave Symposium Digest*, 2023.
- [31] N.-N. Dao et al., "A review on new technologies in 3GPP standards for 5G access and beyond," *Computer Networks*, vol. 245, p. 110370, 2024.
- [32] R. Lu and S. Gong, "RF acoustic microsystems based on suspended lithium niobate thin films: advances and outlook," *Journal of Micromechanics and Microengineering*, vol. 31, no. 11, p. 114001, 2021.
- [33] N. F. Naumenko, "Enhancement of high-frequency harmonics in resonators using multilayered structures with polarity-inverted layers," *Results Phys*, vol. 65, p. 107998, Oct. 2024.
- [34] R. Lu, Y. Yang, S. Link, and S. Gong, "Enabling Higher Order Lamb Wave Acoustic Devices with Complementarily Oriented Piezoelectric Thin Films," *Journal of Microelectromechanical Systems*, vol. 29, no. 5, 2020.
- [35] V. Chulukhadze et al., "Frequency Scaling Millimeter Wave Acoustic Devices in Thin Film Lithium Niobate," in *IEEE International Frequency Control Symposium (IFCS)*, 2023.
- [36] Microlambda Wireless, "YIG Filter," <https://www.microlambda.com/>.
- [37] RF Lambda, "Waveguide Filter," <https://www.rflambda.com/>.
- [38] CUBIC/Nuvotronics, "3D Print Filter," <https://www.cubic.com/nuvotronics-home-page>.
- [39] Knowless Precision Devices, "Microstrip Filter," <https://www.knowlescapacitors.com/>.

[40] TDK, "LTCC Filter," <https://product.tdk.com/>.

[41] Marki Microwave, "Passive GaAs MMIC Filter," <https://markimicrowave.com/>.



**Omar Barrera** (Student member, IEEE) Omar is a Ph.D. candidate at UT ECE. He graduated with a B.S. degree from UABC in Mexico and an M.Eng. from Dongguk University in Korea, both in Electrical Engineering. He has previous research experience in antennas and RF circuits. He

also has industry experience in the automotive industry, where he worked as a manufacturing engineer. His current research interests involve microwave and mm-wave devices and circuits, and more in particular, the development and characterization of acoustic filters for new radio mobile applications. Omar was the recipient of an Outstanding Student Oral Presentation Award Finalist in IEEE MEMS 2024 and was awarded 2nd place in the Conference Paper Award in IEEE International Microwave Filter Workshop (IMFW 2024). He has also received the Cadence Diversity in Technology Scholarship in 2023.



**Jack Kramer** (Student member, IEEE) received his B.S. from the University of New Mexico in 2021 and is currently pursuing his Ph.D. in electrical engineering at the University of Texas at Austin. His research has focused on millimeter-wave and sub-terahertz acoustic systems leveraging lithium niobate thin films. His interests include the

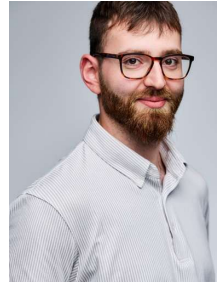
further integration of these systems into hybrid optical and quantum systems. He received best student paper awards at IEEE International Frequency Control Symposium (IFCS) in 2023 and IEEE International Conference on Microwave Acoustics and Mechanics (IC-MAM) in 2022. He also received the 2024 Ben Streetman Junior Researcher Award, the 2025 University of Texas Continuing Fellowship, and the 2025 Texas Quantum Institute Fellowship.



**Lezli Matto** received her B.S. in Materials Science and Engineering from the Polytechnic School at the National University of Asunción in Paraguay in 2017. She received her Master of Science in Engineering in Materials Science and Engineering from the University of Texas at Austin in 2021 funded by the Fulbright

Scholarship. Lezli is currently a PhD candidate in the

Materials Science and Engineering department at the University of California Los Angeles (UCLA). Her research interests focus on wafer bonding, ion implantation, exfoliation and thin film layer transfer for heterogeneous integration, and chemical mechanical polishing (CMP) of semiconductor materials. Additionally, she works with characterization techniques such as High-resolution X-Ray Diffraction (HRXRD) and Transmission Electron Microscopy (TEM).



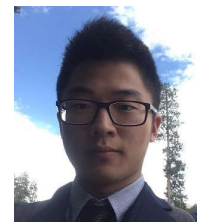
**Vakhtang Chulukhadze** (Student member, IEEE) received his B.S. from the University of Rochester and is currently pursuing his Ph.D. in electrical engineering at the University of Texas at Austin. His research has focused on lithium niobate microsystems spanning a wide range of frequencies and applications. His interests include

further system integration of these piezoelectric components into larger systems for front-end signal processing and sensing. Vakhtang is the Jim and Dorothy Doyle scholar, as well as a Russel F. Brand Engineering Acoustics fellow, and Professor Edith Clarke fellow. He received an outstanding poster award at the Hilton Head workshop 2024 alongside the Ben Streetman award in graduate research on electronic and photonic devices.



**Sinwoo Cho** (Student member, IEEE) is a Ph.D. candidate at UT Austin ECE. He received his B.S. degree in Biomedical Engineering from Inje University, Korea, in 2019 and his M.S. degree in Integrated Design Engineering from Keio University,

Japan, in 2021. His research primarily focuses on RF acoustic front-end, including RF microsystem, RF MEMS, filter, and resonator. He received the Microwave Theory and Technology Society (MTT-S) Graduate Fellowship 2025, IEEE International Microwave Symposium third place Best Student Paper Award in 2024, IEEE Micro Electro Mechanical Systems (MEMS) Best Student Paper Finalists in 2021, and 2024 respectively, Qualcomm Innovation Fellowship (QIF) North America Finalists in 2022, and IEEE Texas Symposium on Wireless & Microwave Circuits and Systems (WMCS) Student Research Competition 1st Place Award in 2022.



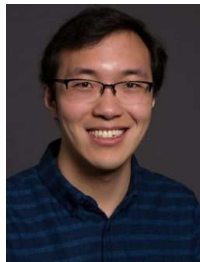
**Michael Evan Liao** is a research scientist at Apex Microdevices. Dr. Liao received his B.S. degree in Chemistry (2017), B.A. degree in Ethnomusicology Jazz Performance (2017), M.S. degree in Chemistry (2017), and Ph.D. in Materials Science



& Engineering (2022) at the University of California Los Angeles. His research aims to develop commercial-compatible solutions towards fabricating composite wafers via wafer bonding of various semiconductor materials including, but not limited to,  $\beta$ -Ga<sub>2</sub>O<sub>3</sub>, SiC, and LiNbO<sub>3</sub>. He received the IUCr Young Scientist Award in 2019 issued by the International Union for Crystallography at the ICCGE-19/OMVPE-19 conference and also the Best Student Paper Award in 2018 at the AiMES 2018 conference (Electrochemical Society). Dr. Liao joined Apex Microdevices after his tenure as a National Research Council Postdoctoral Fellow at the U.S. Naval Research Laboratory, Washington, DC.



**Mark S. Goorsky** received his B.S. degree from Northwestern University in 1984 and his Ph.D. from the Massachusetts Institute of Technology in 1988. He has been on the faculty at UCLA since 1991 and was department chair from 2005-2010. His research focuses on wafer bonding, layer exfoliation and transfer, and chemical mechanical polishing of semiconductors and optical materials. Goorsky also provides expertise in materials characterization of semiconductor materials and devices, with emphasis on structural (x-ray scattering and electron microscopy) and chemical (electron energy loss spectroscopy, energy dispersive elemental analysis) techniques. His current research areas include materials integration of wide bandgap semiconductors and thin film electro-optic-acoustic materials such as lithium niobate. Goorsky received the university-wide 2016 UCLA Distinguished Teaching Award and the Harvey L. Eby Award for the “Art of Teaching”, was a member (2011-2015) of the US Air Force Science Advisory Board, was (2002-2019) associate editor for the Journal of Crystal Growth, was awarded the T.S. Walton Award from the Science Foundation of Ireland in 2010 and received (1995-2000) a National Science Foundation Career Award.



**Ruochen Lu** (Senior Member, IEEE) is an Assistant Professor in the Department of Electrical and Computer Engineering at The University of Texas at Austin. He received the B.E. degree with honors in microelectronics from Tsinghua University, Beijing, China, in 2014, and the M.S. and Ph.D. degree in electrical engineering from the University of Illinois at Urbana-Champaign, Urbana, IL, USA, in 2017 and 2019, respectively. His research primarily focuses on developing chip-scale acoustic and electromagnetic components and microsystems for RF applications. His works aim to demonstrate RF MEMS platforms, toward higher operating frequencies and more efficient transduction between the

EM and acoustics. In addition, he works on ultrasonic transducers and multi-physics hybrid microsystems for signal processing, sensing, and computing applications. He received IEEE TC-S Microwave Award in 2022, IEEE Ultrasonics Early Career Investigator Award in 2024, and NSF Career Award in 2024. Along with his students, he received Best Student Paper Awards at IEEE International Frequency Control Symposium (IFCS) 2017 and 2023, IEEE International Ultrasonics Symposium (IUS) 2018 and 2022, IEEE International Conference on Microwave Acoustics & Mechanics (IC-MAM) 2022, and third place Best Student Paper Award at IEEE International Microwave Symposium (IMS) 2024. He received the Junior Faculty Excellence in Teaching Award in 2024 from the University of Texas at Austin. He is an associate editor of IEEE Journal of Microelectromechanical Systems, IEEE Transactions on Ultrasonics, Ferroelectrics, and Frequency Control, and a topic editor of IEEE Journal of Microwaves.